



In situ crystallization of non-cotectic and foliated igneous rocks on a magma chamber floor

Willem Kruger ¹✉ & Rais Latypov ¹

Layered mafic intrusions commonly contain non-cotectic, foliated igneous rocks that are traditionally attributed to processes involving settling, transport, and redeposition of crystals. Here we examine the chemistry of magnetite layers of the Bushveld Complex using a portable XRF spectrometer on drill core and dissolution ICP-MS analysis on pure magnetite separates. While magnetites contain foliated plagioclase grains in non-cotectic proportions, the magnetite is characterized by a regular upwards-depletion of Cr which is best explained by in situ crystallization. We suggest that plagioclase nucleation in thin residual compositional boundary layers atop a solidification front causes in situ growth of plagioclase in proportions much lower (<10%) than those expected from cotectic crystallization ($\pm 85\%$). Crystallization in such a boundary layer also favours lateral growth of the plagioclase, producing the foliation. We suggest that some non-cotectic, foliated rocks that are commonly interpreted to arise from gravity-induced sedimentary processes may instead be produced by in situ crystallization.

¹School of Geosciences, University of the Witwatersrand, Johannesburg, South Africa. ✉email: Willem.Kruger@wits.ac.za

Fossilized basaltic magma chambers are commonly characterized by intricate layers of igneous rocks that preserve important clues for deciphering magmatic processes. For decades, these layered intrusions served as important natural laboratories for investigating how basaltic melts crystallize and differentiate^{1–3}. Unraveling the crystallization histories of magma chambers has, however, proven to be a difficult task, with much debate revolving around layer-forming mechanisms⁴. A key aspect to this discussion is how crystals accumulate in magma chambers. One common idea is that crystals nucleate and grow at the chamber margins in structures called solidification fronts^{5–13}. This may either occur by heterogeneous nucleation, where crystals nucleate against the country rock or pre-existing mineral grains^{5,12}, or homogenous nucleation, where crystals nucleate within the melt in the vicinity of the margins of the intrusion⁶. With progressive cooling of the intrusion, solidification fronts will advance inwards towards the chamber interior until the chamber is entirely solid⁹. This process, where crystals remain in their original position after formation, is called *in situ* crystallization, and the resulting rocks may be characterized by certain features: if there is effective fractionation between crystals and liquid during crystallization, co-crystallizing primocrysts (i.e., early-formed mineral grains that do not crystallize from the interstitial melt) are expected to occur in cotectic proportions as predicted by mineral phase equilibria¹⁴ (Fig. 1a). Grains may have random orientations (e.g., randomly oriented chromite grains nucleating heterogeneously on overturned contacts¹⁵), unless large compositional gradients are present¹⁴.

However, it is not uncommon for layered intrusions to have rocks that do not contain cotectic proportions of primocrysts¹⁶. Good examples of non-cotectic rocks can be found within the Critical Zone of the Bushveld Complex or the Peridotite Zone of the Stillwater Complex, where orthopyroxene, plagioclase, and chromite (Bushveld)^{16,17} or olivine and chromite (Stillwater)¹⁸ occur in widely varying proportions. Such primocrysts may also display a very limited range in grain size and show a foliation that is parallel to the bedding plane¹⁹. To produce these latter features, a consensus exists that these primocrysts must have undergone some type of hydrodynamic sorting. This may include crystal settling^{1,20–22}, flotation²³, transport or re-arrangement by magma currents^{19,24–27}, intrusion of crystal mushes from deeper-seated magmatic bodies^{16,28–30}, or re-arrangement of crystal mushes by tectonic disturbances³¹. Movement of crystals by whatever mechanism tends to sort them by size¹⁴, and the process may produce a magmatic foliation and/or lineation in the case of elongated mineral grains^{25,26,32}. Since such a process may also sort minerals by density, it may lead to rocks with cumulus mineral proportions that deviate dramatically from the expected cotectic proportions^{30,31} (Fig. 1b, c).

In this contribution, we present an intriguing case from the Bushveld Complex in South Africa in which layers of magnetite bear a perplexing mixture of characteristics, some of which are suggestive of *in situ* crystallization, while others argue for crystal sorting. Bushveld magnetite layers are characterized by a smooth and extremely rapid depletion of their Cr contents

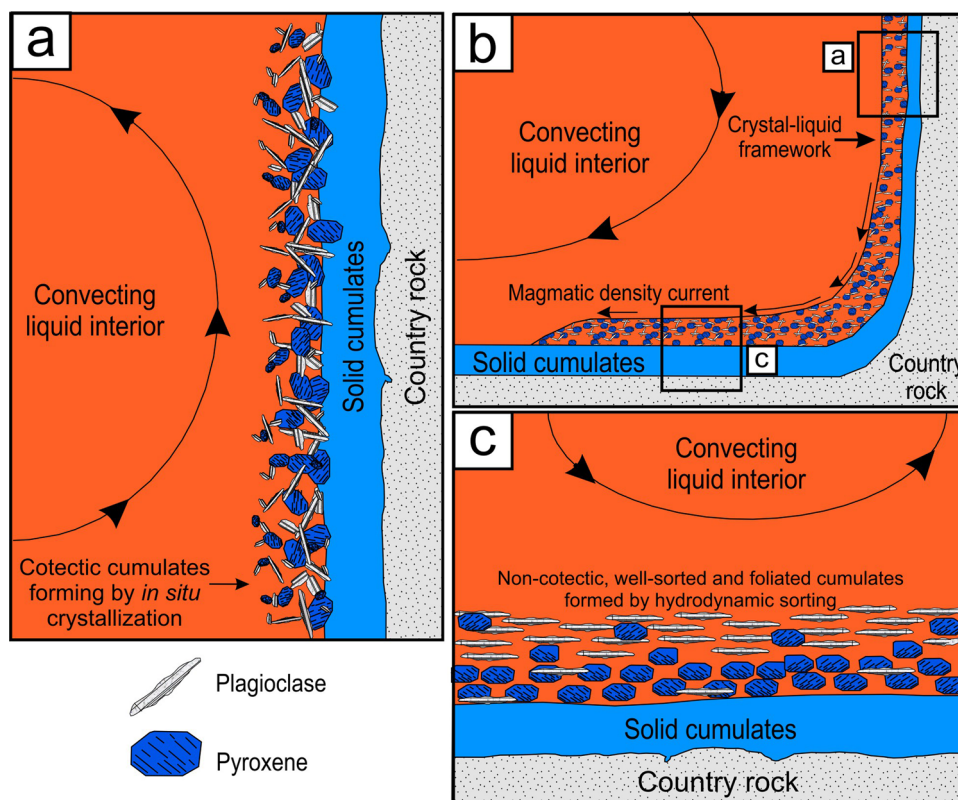


Fig. 1 A magma chamber model for the common case where a basaltic melt crystallizes plagioclase and pyroxene to illustrate the differences that may arise in primocrysts that accumulate by *in situ* growth versus those that are transported. **a** Diagram shows the wall of a magma chamber where heat loss through the country rock results in the nucleation and growth of crystals at the chamber margin and eventually on each other (*in situ* crystallization). With time, this results in a rock that has a large assortment of grain sizes with random orientations in more or less cotectic mineral proportions. **b** In some instances, the crystals on the chamber wall may become unstable, causing them to collapse and flow downwards as a density current to and along the chamber floor²⁷. **c** This flow of the crystal mush may cause grains to become sorted by size and density, leading to rocks with non-cotectic proportions of minerals that may also display a well-developed foliation. While this example illustrates crystal transport by a density current, the same effect can also be achieved by other means, for instance, by gravity settling of crystals from the chamber interior following their homogeneous nucleation.

upwards, from as high as 40,000 ppm at their bases³³ to just 1000 ppm at their tops across a vertical distance of just 1 m⁷. Such a depletion is thought to originate primarily due to the fractional crystallization of magnetite from a limited volume of liquid^{7,13,34} and the extremely high crystal–liquid partition coefficient of Cr into magnetite (from 20 to 600 in basaltic systems to beyond 1000 in more evolved systems^{7,13,34–40}). The remarkable regularity in the depletion suggests that settling was not an important factor to produce a magnetite layer, as a homogenous compositional profile would then be expected⁷. In addition to the above, dome-shaped, high-Cr structures were documented at the bases of these layers that were interpreted as indicating the sites of incipient nucleation and growth of magnetite, supporting the idea that magnetite layers crystallize predominantly by in situ growth^{13,33}. An alternative explanation for the high-Cr structures have recently been proposed where these structures are interpreted to form by the upward-migration of Cr-rich interstitial melt from the underlying cumulate pile⁴¹. However, this model is not consistent with field observations. At the Magnet Heights locality, a basaltic xenolith of about 0.6 m thick and 30 m long, underlies one of the Bushveld Complex’s magnetite layers. This xenolith served as an impermeable barrier to melt/fluids migrating from below⁴². However, the Cr values within the magnetite layer where it drapes over the xenolith falls within the range of values recorded in the magnetite that is not underlain by the xenolith⁴². This suggests that an interstitial liquid percolating upwards from the underlying cumulates did not affect the Cr distribution of magnetite layers, favouring of the original hypothesis of the Cr-rich structures as in situ crystallization phenomena³³.

Despite the evidence for a limited contribution of crystal settling to the origin of magnetite layers, some intervals of these layers contain notably non-cotectic proportions of foliated plagioclase crystals. Almost all magnetite layers of the Bushveld Complex are also characterized by a gradational top into an overlying magnetite–anorthosite layer. Here, we have further documented the distribution of Cr across sections where the mineralogy and texture are suggestive of crystal settling and redeposition and found that exceptionally regular and rapid upwards depletions in Cr occur across these intervals. To our knowledge, no model has yet been presented that can reconcile all these observations. In this study, we propose a model to explain how non-cotectic, foliated primocrysts may arise by the process of in situ crystallization. The solution to the problem lies within thin (a few mm) compositional boundary layers that arise atop the magnetite solidification front¹³. Extraction of magnetite components to form the liquid boundary layer around in situ growing magnetite may lead to the nucleation and growth of plagioclase feldspar within this layer. Continuous removal of the boundary layer by compositional convection, however, causes plagioclase to grow in a lower abundance than predicted by the plagioclase–magnetite cotectic. The growth of magnetite also causes a compositional gradient to develop across the boundary layer, and a greater degree of plagioclase-forming elements become available directly adjacent to the solidification front. This favors the lateral growth of plagioclase, producing a magmatic foliation by in situ crystallization.

Results and discussion

Magnetite layers of the Bushveld Complex. The layered, ultramafic to monzonitic part of the Bushveld Complex in South Africa^{43,44} generally appears to have undergone a tholeiitic trend of differentiation, complicated by the intrusion of multiple magma batches, with Fe-enrichment eventually leading to the appearance of magnetite primocrysts in the intrusion’s Upper

Zone. It is within this part of the complex that magnetite layers (>90% titanomagnetite) are found (Fig. 2). Drill core from the Rhovan and Vametco vanadium mines in the Western Limb of the Bushveld Complex (Supplementary Fig. 1) served as the primary source of information for this study. Two prominent magnetite layers were targeted to document their textural and geochemical characteristics: the Bottom Seam (BS), which is the lowermost magnetite layer that occurs within this part of the Bushveld Complex, and the Main Magnetite Layer (MML), which occurs about 170 m higher up in the stratigraphy. These layers typically range from 50 to 200 cm in thickness. They are separated by thick swaths of largely homogeneous magnetite-bearing gabbroic rocks, with subordinate, usually thin, anorthositic and magnetite layers occasionally present.

Magnetite layers are typically characterized by a mottled anorthositic footwall, an almost completely massive part consisting of titanomagnetite, and an upper gradational contact, typically transitioning into magnetite–anorthosite (Figs. 2 and 3a). Plagioclase grains are dispersed throughout the typically more massive portions of magnetite layers and are occasionally concentrated in layers typically no more than a few cm in thickness (Fig. 3a). These plagioclase grains typically do not exceed modal proportions of 10%. In the upper gradational portion of magnetite layers, there is a rapid increase in the modal proportion of plagioclase from less than 10% to about 80% across just a few to a couple of tens of centimetres (Fig. 3a).

Plagioclase grains commonly display tabular grain shapes, although they appear to become more equant in the anorthosite located directly above the magnetite in some cases (Figs. 3–5). There is a large range in grain sizes in plagioclase, from <1 to 5 mm (Fig. 3d). The smallest of plagioclase grains can be seen as dots of light in Fig. 3b and may be largely altered. Elongated grains typically display a moderate to well-defined foliation (Figs. 3–5), although some grains can be oriented normal to the general foliation plane. Sub-parallel alignment of albite twins amongst plagioclase grains also shows some degree of a crystallographic alignment, and the b-axis is generally perpendicular to the magmatic layering (Fig. 3d) (Supplementary Fig. 2) (Supplementary Data 1). Importantly, no lineation of plagioclase crystals is evident from visual inspection of both outcrops and individual samples due to their equant habits when viewed from above (Fig. 2c–e).

Cr distribution across magnetite–plagioclase cumulates. We have built here upon pioneering studies by Cawthorn and McCarthy^{7,8,45,46} by documenting the distribution of Cr in magnetite across sections containing non-cotectic proportions of plagioclase grains (“Methods” and Supplementary Data 2). The distribution patterns of Cr in magnetite are believed to be a primary magmatic feature, as discussed in several previous studies^{7,13,33}. The two portions of magnetite with plagioclase crystals within the layer documented here generally shows a very smooth upward depletion (Fig. 4).

A smooth upward depletion has been also documented for a very thick upper gradational contact for the MML (Fig. 5a), although it is possible that the larger sample spacing employed here missed some irregularities. A very detailed analysis across the 13 cm thick upper gradational contact of the BS via ICP-MS reveals the most noteworthy observation of this study. A very rapid but remarkably smooth depletion in Cr upward (Fig. 5b) is observed across this contact (“Methods”), despite the fact that it contains non-cotectic proportions of foliated plagioclase grains.

Crystal sorting to produce non-cotectic plagioclase–magnetite cumulates. The exact cotectic proportions between magnetite and

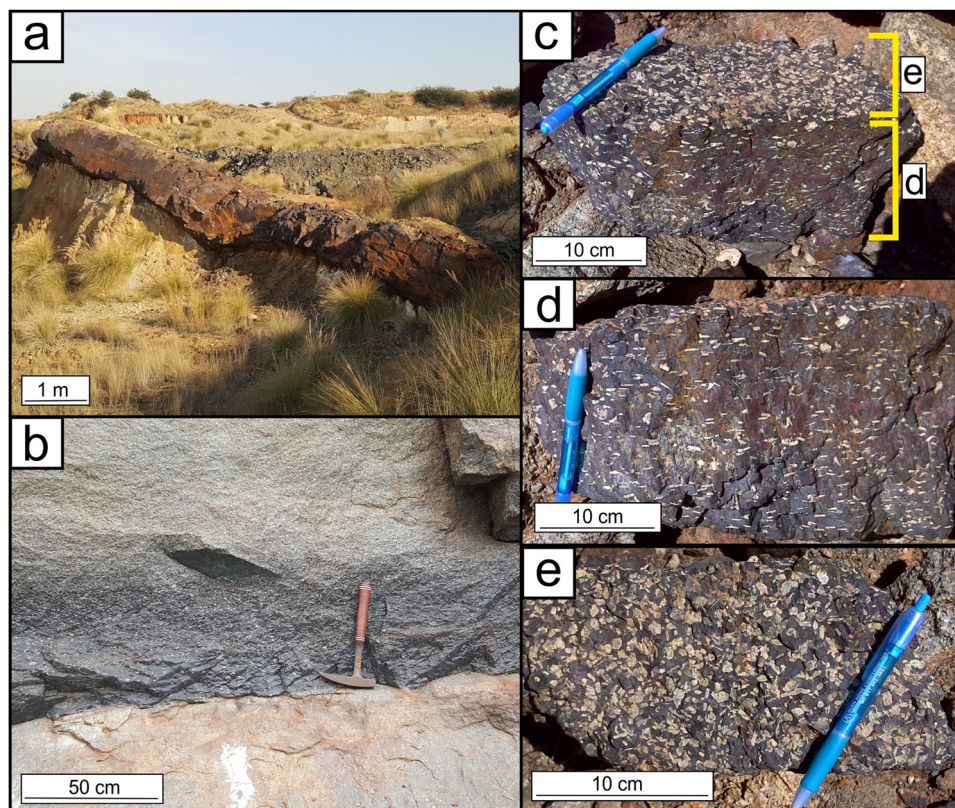


Fig. 2 Appearance of magnetite layers from the Bushveld Complex. **a** An exposure of the main magnetite layer (MML) from the Rhovan mine in the Western Limb providing a three-dimensional perspective on the appearance of the layer. The layer is about 1 m thick. **b** Magnetite Layer 1 from Magnet Heights in the Eastern Limb located about 2 m above the MML. The layer displays remarkable modal layering as it grades into overlying magnetite–anorthosite via non-cotectic proportions of plagioclase and magnetite. Notice the light-colored anorthositic footwall. Hammer is 40 cm in length. **c** A sample of a magnetite layer containing plagioclase grains from the Mapochs Mine in the Western Limb. **d** The same sample as (**c**) viewed from the side to demonstrate the well-foliated nature of the plagioclase. **e** The same sample viewed from above. Plagioclase grains appear more equant, and no lineation is evident from visual inspection.

plagioclase are not known. However, some idea of what it might be can be obtained from observations from various layered intrusions around the world. For example, 7–10% magnetite is observed in the Muskox intrusion in association with plagioclase and pyroxene⁴⁷. In the Sept Iles Complex, gabbroic rocks contain, on average, 15–20% of magnetite and ilmenite in gabbroic rocks¹². Since magnetite appears to crystallize in a proportion of about 2:1 to ilmenite⁴⁷, the actual cotectic proportions for magnetite for Sept Iles rocks may be even lower (around 10–15%). For the Bushveld Complex, the cotectic proportion of magnetite has been estimated to be around 8% to silicate minerals^{48,49}. When magnetite crystallizes with plagioclase but in the absence of pyroxene, this value is likely to be somewhat higher. Experimental studies⁵⁰ recorded a higher cotectic proportion of magnetite to plagioclase and pyroxene of about 22% in anhydrous melt at conditions close to FMQ. In any case, the high proportions of magnetite (>90%) compared to plagioclase within the layers is extremely unlikely to represent cotectic proportions of these two minerals. The upper contacts of magnetite layers also must grade across non-cotectic ratios of magnetite and plagioclase. Such features are commonly explained by models involving crystal sorting. Four major possibilities can be considered below.

The first model considers the deposition of a suspension of magnetite and plagioclase from a melt that may either have crystallized a cotectic assemblage of magnetite and plagioclase, possibly kept afloat by convecting melt overhead the chamber floor, or a plagioclase–magnetite slurry that is injected into the magma chamber. As these crystals settle out on the chamber

floor, they become sorted by density. Since Bushveld magnetite has a much greater density (4.8 g/cm^3)⁵¹ compared to plagioclase (ca. 2.7 g/cm^3), it may sink faster, creating a layer that is enriched in magnetite relative to the cotectic^{29,49,52}. Tranquil settling of plagioclase crystals may cause them to become aligned to produce the foliation. However, a suspension of magnetite crystals will be in equilibrium with the melt and therefore all crystals will have the same Cr concentration. Thus, when a cotectic suspension of magnetite and plagioclase settles out over a sufficient distance to properly separate them into non-cotectic proportions, the magnetite should have a constant concentration throughout. However, what is observed in reality is a rapid and regular decrease in Cr upwards (Figs. 4 and 5). There are also no signs that plagioclase grains were sorted by size, as both the magnetite and overlying magnetite–anorthosite show great internal variation in plagioclase grain size.

In the second model, we can consider short-distance settling of magnetite and plagioclase crystallizing directly ahead of a solidification front⁷. However, both these settling models requires that magnetite sinks faster than plagioclase. Although present-day magnetite grains are large (1–2 cm)⁵³, magnetite inclusions in silicates are much smaller ($\pm 0.007 \text{ mm}$) and are thought to represent the original grain size of magnetite grains that were shielded from post-accumulation annealing⁵⁴. Since grain size exerts a much large influence on settling rates than density, it is only for a very restricted range of liquid density ($2704\text{--}2710 \text{ kg/m}^3$) where plagioclase grains (with radii that commonly exceed 0.12 mm) would sink slower than magnetite (Supplementary Data 3

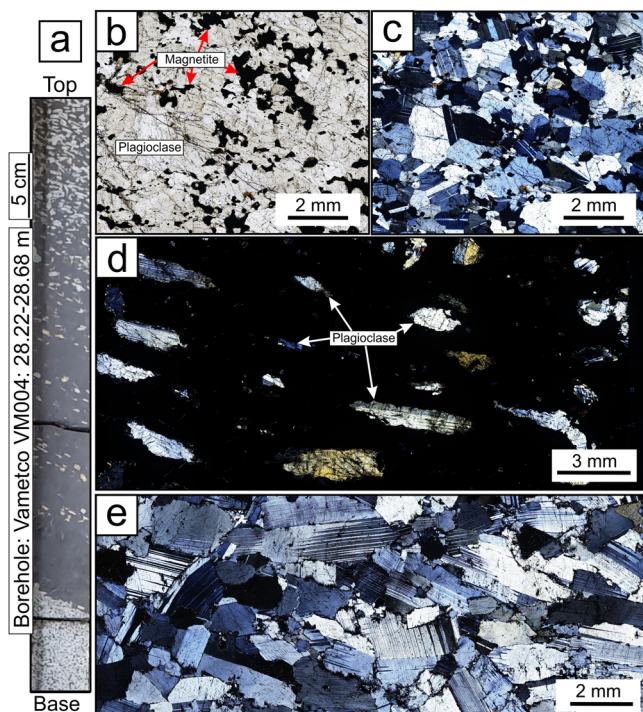


Fig. 3 Appearance of magnetite and adjacent lithologies. **a** A relatively thin magnetite layer sampled in drill core from the Vametco mine in the Western Limb. The layer shows characteristics that are common to most magnetite layers of the Bushveld Complex. These include a light-colored anorthositic footwall, a dark gray magnetite layer with a sharp and perfectly massive base with sporadic occurrences of moderate to well-foliated plagioclase primocrysts (light in color) further upwards, and an upper gradation into a plagioclase-rich layer. **b** Photomicrograph of the overlying magnetite-anorthosite in plane-polarized and **(c)** crossed polars. The grain size of plagioclase varies substantially, they tend to be mostly equant to occasionally tabular in shape, and a foliation appears weak or absent. **d** Photomicrograph of the upper gradational contact of a magnetite layer shown in Fig. 5b. Plagioclase grains, surrounded by Fe-Ti oxides, are tabular with irregular boundaries. A well-developed foliation can be observed, while the sub-parallel orientation of albite twins hint at a crystal-preferred orientation (crossed polars). **e** Photomicrograph of the footwall anorthosite. Plagioclase grain size is variable, grain contacts are planar to irregular, with indications of deformation. All thin sections are oriented perpendicular to the igneous layering.

and Supplementary Fig. 3; “Methods”) to produce the gradational contacts. The dramatic differences in grain size of the plagioclase grains is also problematic. Different plagioclase grains will sink at dramatically different rates, and for them to accumulate in the same layer they will have to sink out over very short distances of just a few cm. It is unlikely that a non-cotectic assemblage of magnetite and plagioclase could arise from such short settling distances.

For the third model, one may consider a situation in which magnetite grew in situ, while plagioclase was deposited on an advancing magnetite solidification front from the overlying melt. In contrast to the first model, this scenario still has the potential to produce a regular Cr depletion upwards, while potentially producing non-cotectic proportions of plagioclase and magnetite. However, this model faces the problem that plagioclase would have to nucleate homogeneously in the chamber interior and settle out, instead of crystallizing directly at the contact of the magnetite solidification front. The latter process is kinetically much more likely to occur^{5,12}. If the magnetite is forming by heterogeneous nucleation, then there is no clear reason

as to why the plagioclase grains would be forming by homogeneous nucleation. Alternatively, plagioclase may be introduced into the chamber as a crystal mush²⁹ during magmatic recharge that settles out on the growing magnetite layer. If such a mush were to settle out over the large time-scales required for a magnetite layer to grow (potentially a few decades according to growth rates inferred for magmatic intrusions⁵⁵), the Stokes’ law predicts that the grains should become sorted by size. As mentioned above, this is not evident from petrographic observations.

All of the above models assume that plagioclase has a higher density than the melt and will therefore tend to sink. However, it is not obvious if plagioclase would be able to sink or float in the parental melt of the Upper Zone of the Bushveld Complex. Based on an estimated parental melt for the Upper Zone⁵⁶, Cawthorn²² stated that plagioclase may float as long as the melt was relatively anhydrous (<1.0 wt. % H₂O). Because of the possibility of plagioclase floatation, it is important to consider if the floating plagioclase can produce the textural and geochemical features of the magnetite layers.

In the fourth model, plagioclase is considered to have floated upwards from the solidification front to accumulate at some upper boundary layer in the liquid. Such a boundary layer could arise by double-diffusive convection³⁴, or it could be the top of a basal flow of magma that entered the chamber^{13,28}. However, the next magnetite-rich layers are located only a few meters above the BS and MML, which would severely limit the amount of liquid from which the magnetite could have crystallized. Vanadium concentrations across vertical profiles in magnetite layers have been observed to be more or less constant⁵⁷ despite high partition coefficients for vanadium in magnetite. To accurately model a rapid decrease in Cr contents while keeping V contents more or less constant, a layer of liquid is needed that is, at least, tens of meters thick^{7,13,34}. A floating model also suffers from the lack of grain sorting by size as the above settling models.

In addition to the arguments presented above, another obstacle for settling models arises from geochemical modeling. Numerous studies have now highlighted the fact that simple fractional crystallization alone cannot explain the variation in Cr along vertical sections across magnetite layers^{7,13,34,41}. The same appears to be true for their upper gradational contacts. Two parameters are unknown when performing geochemical modeling, namely the thickness of the liquid layer the magnetite is crystallizing from, and the exact partition coefficient of Cr in magnetite. These parameters can be altered to obtain the best fit with real chemical data. For the modeling, we can consider two scenarios (Fig. 6 and Supplementary Data 4) based on the sample shown in Fig. 5c. In the first scenario, magnetite and plagioclase are crystallizing in cotectic proportions, and the gradational contact is produced by crystal settling. If we assume a D value for Cr in magnetite is 300, and a cotectic proportion of 10% of magnetite to plagioclase, this will result in a bulk D value of 30. To produce a depletion across the upper gradational contact (Fig. 5c), a liquid layer of about 5 m thick is required, although the modeling results do not fit properly with the real data. In fact, a poor fit is always produced when a constant D value is used. In the second scenario, the assumption is made that the magnetite and plagioclase are crystallizing in situ, so that the abundance of magnetite and plagioclase observed in the gradational contact are the true abundances that are being extracted from the liquid. In this case, the whole-rock D value decreases in a manner that corresponds to the increase in the plagioclase mode, and a much better fit can be obtained (this time using a much thicker liquid layer of 41 m). Of course, there are many other ways in which a better fit with the data may be produced that range from models involving chemical diffusion^{7,34}, multiple episodes of magmatic

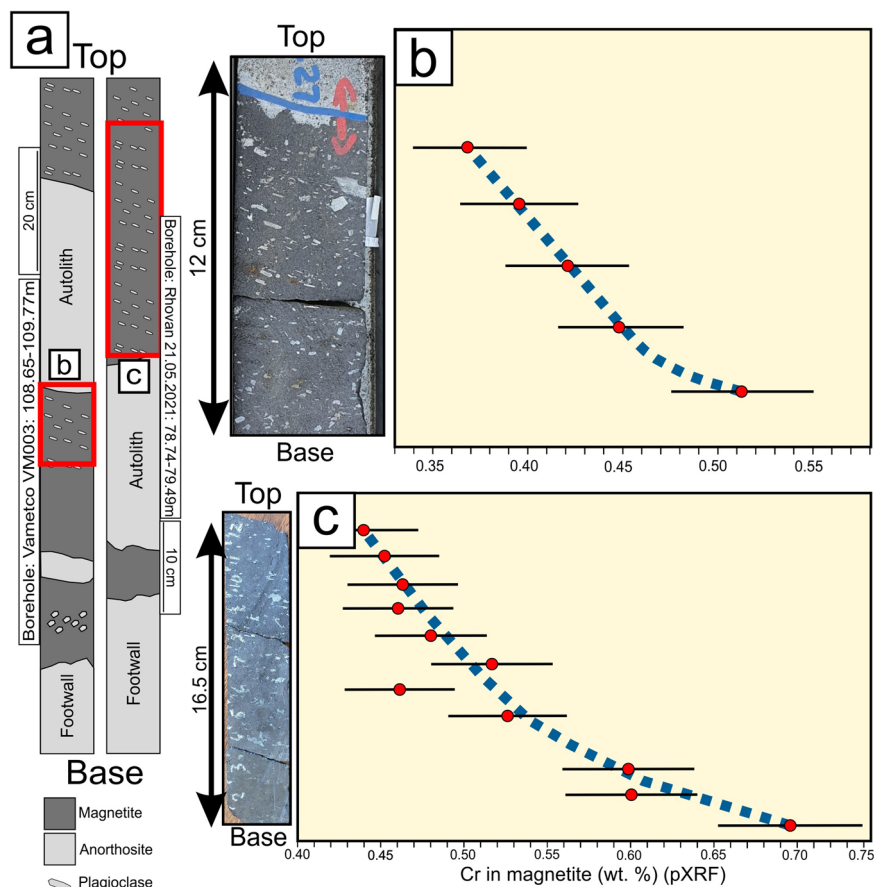


Fig. 4 Cr in magnetite analyzed across two portions of the bottom seam from the Vametco mine in the Western Limb that contain plagioclase primocrysts. Sections were analyzed using a portable XRF spectrometer (“Methods”). **a** Sketches of drill cores with the sections analyzed are highlighted in red. The light-colored anorthositic footwall is shown in both examples and is overlain by dark magnetite. Both examples contain light-colored anorthositic autoliths. In **b**, **c** the distribution of Cr in magnetite is shown across sections containing non-cotectic portions of magnetite and plagioclase. A steep, but regular upward depletion is observed in both cases. Horizontal lines indicate 2σ error bars on both **b**, **c**. Blue lines are fit by hand to highlight the trend of Cr depletion.

recharge and mixing¹³, or a decrease in the effectivity of crystal–liquid exchange⁴¹. However, these results suggest that the proportions of magnetite and plagioclase observed in the gradational contact represent the true proportions that are crystallizing from the melt, and that magnetite and plagioclase are not being crystallized in the expected cotectic proportions.

The above gravity settling models and those combining elements of both gravity settling and in situ crystallization are thus unable to explain the non-cotectic proportions of plagioclase and magnetite while accounting for the regular depletion in Cr observed across these layers. Thus, it seems that a different model is required to reconcile all these observations.

In situ crystallization of non-cotectic cumulates. Before a solution can be provided for this problem, a brief review is required of the processes operating prior to and during magnetite crystallization, as discussed in our recent studies^{13,58}. At first, a melt is required at the chamber floor that is saturated in magnetite-alone. Magnetite-alone saturation may be achieved in numerous ways that include a pressure increase in the chamber due to tectonic activity⁷, a pressure reduction experienced by magma as it rises through the crust⁵⁹, liquid immiscibility^{54,60}, among many others. A discussion of which model is most plausible is beyond the scope of the current study. Whatever the case may be, this melt crystallized magnetite in situ on various spots on the chamber floor. Magmatic differentiation was

operative almost immediately after crystallization started by the convective removal of extremely thin liquid boundary layers from the growing crystals. These compositional boundary layers arise during diffusion of magnetite-building components through the melt towards the growing crystals, resulting in a melt layer that has a relatively lower density compared to the overlying melt. This boundary layer will break away convectively from the solidification front once it reaches some critical thickness (about 1.7 mm) and density (a change of 14.5 kg m^{-3} compared to the overlying liquid)^{13,61}. The vigorous convection of the boundary layer results in extremely effective accumulation growth of the magnetite, causing the solidification front to propagate as an essentially solid surface^{13,58}. Since the magnetite layers are overlain by magnetite–anorthosite, plagioclase is the second phase that comes to the liquidus after some fractional crystallization has occurred.

Based on this information, we propose a model for the origin of non-cotectic cumulates by in situ crystallization (Fig. 7). As magnetite components are extracted from the overlying liquid, it results in a boundary layer that becomes increasingly richer in plagioclase components until it is light enough to convect. The boundary layer may break away as a constant stream of melt or as a series of plumes^{61–64}. While it is not clear what convective style will dominate, for the model presented here to work, we must assume that the boundary layer breaks away periodically as a series of plumes.

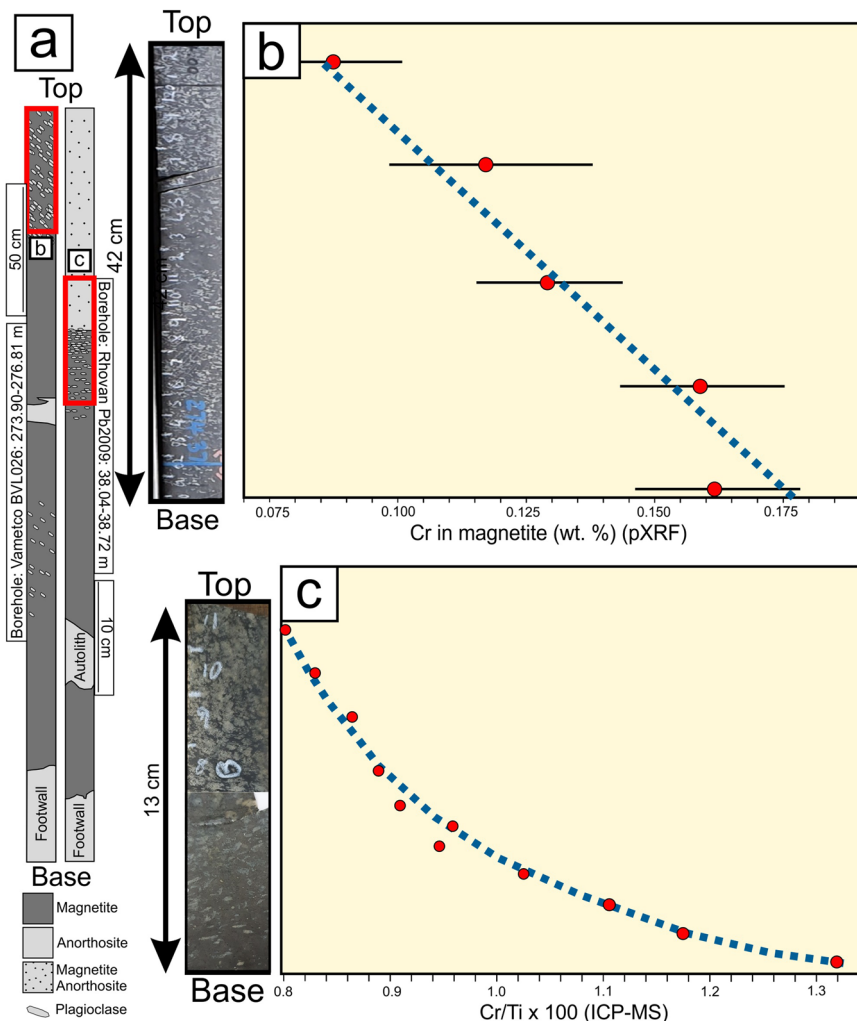


Fig. 5 Cr in magnetite across the upper gradational contacts of magnetite layers from the Vametco mine in the Western Limb. **a** Sketches of drill cores with the analyzed sections highlighted in red. As in Fig. 4, the anorthositic footwall can be seen in both examples and anorthositic autoliths are present in both magnetite layers. A complete gradation to magnetite–anorthosite can be seen atop the Bottom Seam (BS) in the Rhovan drill core. **b** A rapid but regular depletion in Cr upwards is observed across a thick gradational contact of the MML from Vametco. Horizontal lines indicate 2θ error bars. **c** Detailed analysis across the upper gradational contact of the Main Magnetite Layer from Vametco. Notice the steep, but remarkably regular depletion in Cr upwards. Cr/Ti ratios are plotted to exclude any feldspar contamination that may be present (methods). Error bars (2θ) for these analysis are too small to show on the figure. Blue lines are fit by hand to highlight the trend of Cr depletion.

At first, although the boundary layers become enriched in plagioclase component, they do not reach plagioclase saturation, resulting in the magnetite monomineralic bases of the BS and MML. As each boundary layer breaks away and mixes with the overlying liquid, this overlying layer becomes increasingly richer in plagioclase component. Mixing of the boundary layer with overlying liquid is necessary to enable its eventual saturation in plagioclase. This process also causes each successive boundary layer that forms to become ever so slightly closer to plagioclase saturation (Fig. 7b). The enrichment of the melt in plagioclase due to magnetite extraction is demonstrated by MELTS modeling in Supplementary Data 5 (“Methods”).

The exact point on the phase diagram⁶⁵ (Fig. 7b) at which the boundary layer breaks away is not clear. In Fig. 7, this is shown to occur just before the boundary layer reaches the magnetite liquidus. The exact thermal behavior of the boundary layer is also not known. It may heat up due to the release of latent heat, or it may cool down if heat loss is sufficiently rapid. These details are not essential for the model, and the boundary layer is illustrated to be isothermal. However, what is required is that

some heat is lost between the removal of each successive boundary layer to allow continuous nucleation of magnetite. This may occur by heat loss through the floor⁵⁸ or through the upper boundary of a hot basal melt layer that arises during magmatic recharge^{13,66}.

At some point, somewhere along the solidification front, a boundary layer will eventually intercept the subsolidus extension of the plagioclase nucleation curve. Initially, the probability of this to happen is low, and likely occurs in isolated spots due to small heterogeneities in the composition of the boundary layer along the solidification front. Once a single nuclei of plagioclase forms, this liquid will be kinetically cooled below the liquidus of plagioclase, and plagioclase growth will dominate. Since extraction of plagioclase components by the nuclei will cause the liquid to immediately evolve away from the nucleation curve, only a single plagioclase grain forms. To sustain the growth of the grain within the very small boundary layer, plagioclase-building components may diffuse from the supernatant liquid downwards into the boundary layer. Alternatively, magnetite growth adjacent to the plagioclase grain will continue to produce melt enriched in

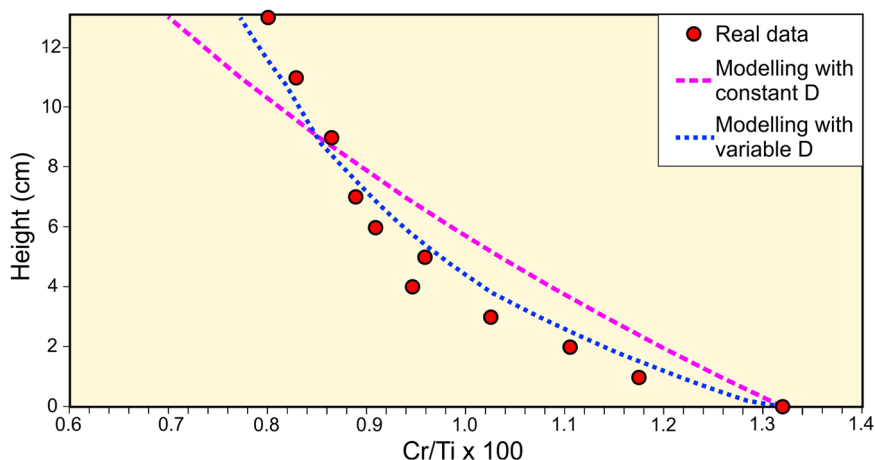


Fig. 6 Geochemical modeling assuming Rayleigh-style fractionation of the variation in Cr across the upper gradational contact shown in Fig. 5c. Using a constant bulk D value for Cr of 30 (assuming a value of 300 in magnetite and a cotectic proportion of 10% of magnetite to plagioclase), a relatively poor match is obtained between the modeling and real chemical data. If the bulk D value is assumed to decrease (from 284 to 89) in line with the increase in the modal abundance of plagioclase (from about 5–70%) observed upwards in the contact, a much better fit with the data can be obtained.

plagioclase components. These components may diffuse laterally through the boundary layer towards the plagioclase grain.

The growth of the plagioclase grain may then be terminated in the following way. Extraction of plagioclase components above the plagioclase grain may force the liquid to evolve back to the magnetite nucleation curve (Fig. 7d). Magnetite will then nucleate and grow on top of the plagioclase grain. Eventually, the grain is completely overtaken by the solid magnetite solidification front.

The above may also explain the irregular grain boundaries of plagioclase (Fig. 3c). The shape of the bottom parts of plagioclase grains would have to conform to small irregularities present in the solid magnetite solidification front below. When magnetite growth starts atop the plagioclase grain, an irregular upper boundary may result if the growth of magnetite is not uniform all along the upper boundary of the plagioclase crystal. The fact that plagioclase does not form oikocrysts (magnetite inclusions in the feldspar are relatively scarce) probably attests to the fact that the solidification front is almost completely solid underneath the grain and becomes entirely solid very quickly when magnetite starts growing on top of the crystal.

At first, the boundary layer will only spend a very short amount of time at the plagioclase nucleation curve before it breaks away convectively. Only very few plagioclase grains would thus be able to form in these early stages. However, as the magnetite and plagioclase nucleation curves converge with further differentiation, plagioclase nuclei become more common, potentially producing the gradational upper contact of magnetite layers.

Thin plagioclase-bearing layers within magnetite (Fig. 3a) probably represent sections where boundary layers start reaching the nucleation curve of the feldspar. However, further magmatic recharge may then terminate feldspar crystallization, as Cr reversals have been documented by previous investigators (by performing in-house X-ray fluorescence (XRF) analysis on pure magnetite separates) above plagioclase-bearing layers⁷. Still, the appearance and disappearance of plagioclase does not always coincide with chemical changes⁴⁶. In these cases, physical changes in the magma chamber, like a drop in pressure, may favor plagioclase crystallization for short periods of time^{7,22,46,49,52}.

Origin of plagioclase foliation. If plagioclase grains grew in situ, we would commonly expect them to have random orientations. Instead, they are characterized by a well-developed foliation within the magnetite (Fig. 3). It is generally accepted that

foliated grains had to become oriented by some process after their initial nucleation and growth. Such processes may include magmatic flow/shear or compaction, and their potential to explain the foliation is explored below.

To produce a foliation by flow, crystals have to be unconsolidated. Perhaps, we can envision a very thin crystal mush, no more than one or two grains in thickness, atop the solidification front that can become oriented by passing magmatic currents. This process can be effective to produce a very well-defined magmatic foliation¹⁹ and potentially also a lineation²⁵, although the latter is not evident from our samples (Fig. 2e). Redistribution of a very thin mush would not disturb the very regular Cr-profiles in magnetite (Figs. 4 and 5). However, magmatic flow would destroy the growth nodes observed at the bottoms of these layers^{13,33}. Perhaps then, magmatic flow only started operating after the growth nodes formed, but there is no clear reason why this should be the case. In addition, heterogeneous nucleation may produce a rigid crystal framework that will be immune to the action of magmatic currents^{12,14}.

Compaction may produce a foliation in one of two ways. It may cause rotation of crystals, so that their long axes become perpendicular to the stress direction, although the process is now considered to be ineffective to produce well-foliated igneous rocks¹⁹. Alternatively, compaction may result in recrystallization to produce a foliation. Tabular grains that are oriented with their long axes perpendicular to the magmatic layering experience much greater stresses during simple shear, causing dissolution on the tops and bottoms of these crystals and redeposition on their sides^{24,67,68}. However, in dealing specifically with magnetite layers of the Bushveld Complex, no textural evidence for compaction for these layers and adjacent lithologies have been found⁶⁰. It has also been suggested that the tabular habit of plagioclase parallel to (010) as observed in this study arises as a primary growth feature, and does not arise during dissolution and recrystallization¹⁴.

There is, however, a group of rocks that grow in situ with non-random orientations. They have been referred to as crescumulates, harristic cumulates, or have been described as comb layering⁴. They form when the melt experiences a substantial amount of undercooling, causing crystals to grow into the liquid interior in search of nutrients to sustain crystallization⁶⁹. Perhaps, a similar process may be responsible for the foliation of plagioclase in our study. However, comb layering is typically expected to develop perpendicular to the magmatic layering, while plagioclase foliation is parallel

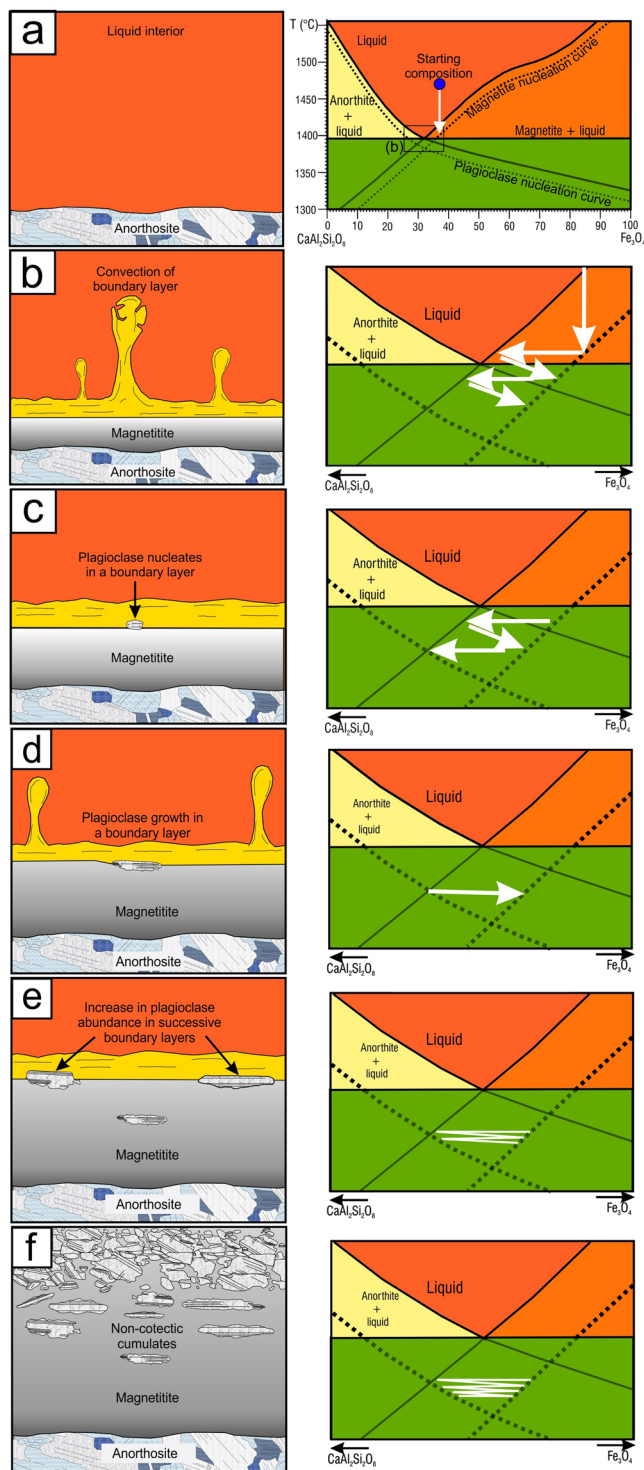


Fig. 7 Cartoons illustrating the process leading to the formation of non-cotectic cumulates by in situ crystallization with corresponding phase diagrams (modified from Roeder and Osborn⁷⁴), showing the evolution of the melt directly at the crystal-liquid interface. The green area on the phase diagram represents the subsolidus. Since the phase relations from Roeder and Osborn are based on atmospheric conditions, they are not directly applicable to the Bushveld Complex that crystallized at greater depth. However, the true-phase relations is not essential for our explanations. The degree of undercooling required for nucleation and the step-wise evolution of the melt is not to scale. **a** Initially, crystal-free liquid overlies an anorthosite layer that is superheated with respect to the magnetite liquidus. Magnetite can only start nucleating and growing once the liquid cools to the magnetite nucleation curve. **b** Once magnetite growth is underway, a thin liquid boundary layer develops overhead the solidification front that is depleted in magnetite component. The boundary layer convects in a plume like fashion, and the plumes eventually undergo mingling and mixing with the overlying liquid. This causes the overlying liquid to become enriched in plagioclase component, and each subsequently forming boundary layer thus becomes slightly closer to plagioclase saturation. **c** At a certain point a boundary layer may finally intercept the plagioclase nucleation curve, so that a plagioclase crystal may start forming. **d** As the plagioclase grows, the liquid adjacent to the grain becomes stagnant due to the extraction of low-density components from the liquid. Crystal growth may be sustained by lateral diffusion of plagioclase-building components from the sides or above. The grain may continue growing until it is eventually overtaken by the solidification front, or if new nuclei of magnetite forms atop the plagioclase grain as the stagnant liquid evolves back to the magnetite nucleation curve. **e, f** With continued liquid evolution, the nucleation curves of magnetite and plagioclase converge. Plagioclase nucleation therefore becomes progressively more common in the boundary layer, and a higher modal abundance of plagioclase results.

is usually the case for crescumulates⁷⁰ and harrisites⁶⁹, is probably because of a lower degree of undercooling experienced by the plagioclase grains in the magnetite.

A final piece of the puzzle is to explain the crystallographic alignment of these crystals (Fig. 3b and Supplementary Fig. 2). Harrisitic olivine crystals from the Rum Complex, that are frequently oriented with their a-axes perpendicular to the magmatic layering, may provide an answer^{69,71}. Because olivine grains grow faster along their a-axes, grains that are oriented with their a-axes at a high angle to the magmatic layering will grow faster than grains with less favorable orientations⁴. Since plagioclase growth proceeds faster along the a- and c-axis in plutonic igneous rocks⁷², a grain of plagioclase that nucleates with these axes parallel to the magmatic layering in a boundary layer would therefore be able to grow faster than unfavorably oriented grains. Unfavorably oriented grains that are only able to grow slowly may even undergo dissolution in favor of faster-growing crystals. The final product is a rock that contains a predominance of tabular plagioclase grains that bear a foliation parallel to the magmatic layering.

The above process may also be able to explain why the tabular habit and foliation becomes lost in the magnetite–anorthosite hangingwall of the BS as observed here (Fig. 3c, d). Later boundary layers will also be richer in plagioclase components throughout with continued fractional crystallization of magnetite. This will cause to the formation of much more abundant plagioclase grains that will impinge as they grow, causing the grains to become more equant in habit.

Conclusion. Non-cotectic, foliated igneous rocks are traditionally explained by processes that involve hydrodynamic sorting of

to it. To understand why this is the case, it is once again necessary to examine what exactly occurs within the liquid boundary layer at the crystal–liquid interface.

Since liquid boundary layers become depleted in magnetite components (Fig. 5b), a situation will arise where the greatest concentration of plagioclase components occurs directly adjacent to the magnetite solidification front (Fig. 8). A grain of plagioclase growing in this environment will thus experience a greater diffusive flux of nutrients from the sides than from directly above. This causes the grain to creep out laterally as it grows, and produces a tabular habit of the grain that appears more equant when viewed from above. The absence of a dendritic habit for the plagioclase, as

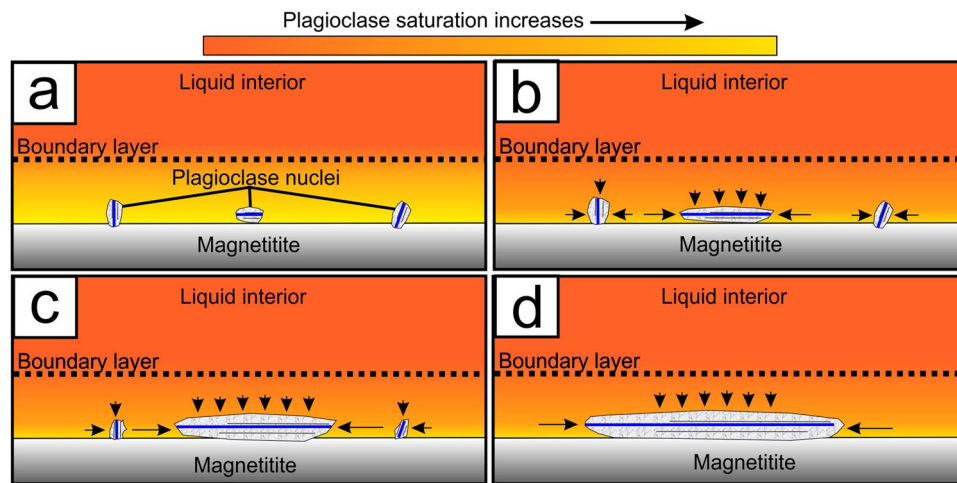


Fig. 8 Origin of foliated plagioclase grains in magnetite. **a** Due to the extraction of magnetite components from the melt during magnetite crystallization, a liquid boundary layer forms with the highest degree of plagioclase saturation (indicated by yellow color) located directly at the crystal–liquid interface. This allows plagioclase grains to nucleate heterogeneously at the bottom of the boundary layer with different orientations. Random orientations for heterogeneously nucleated crystals appear to be possible based on recent observations on chromitite layers¹⁵. Blue lines indicate the orientation of the a-axis of plagioclase grains along which growth is generally faster⁶⁵. **b** As the plagioclase grains start growing, the degree of plagioclase saturation within the boundary layer starts to drop. Since the melt directly above the plagioclase contains a lower concentration of plagioclase components, growth is limited in an upward direction, and the diffusive flux of crystal nutrients (indicated by the size of the black arrows) is greater from the sides. The plagioclase grain in the center with its faster-growing faces oriented perpendicular to the solidification front thus manages to grow faster than the other grains, causing it to become elongated parallel to the a-axis. **c** As nutrients diffuse towards the faster-growing crystal, grains with less favorable orientations begin to dissolve. **d** With time, mostly grains with their a-axis parallel to the solidification front survives.

crystals. This is what makes magnetite layers of the Bushveld Complex so enigmatic, as they clearly possess non-cotectic, foliated cumulates while steep vertical gradients in the Cr concentration strongly argue for in situ crystallization. Since existing models fail to reconcile these observations, it is necessary to come up with new ideas to explain how these magnetite and plagioclase crystals accumulated on the magma chamber floor. We think that the existence of thin compositional boundary layer directly atop the solidification front^{12,61,62} is instrumental to understand these contradictory observations. If these boundary layers are frequently removed by convection, a phase that only reaches saturation in the melt later on will not be able to grow in the abundances predicted by mineral phase equilibria. However, the abundance may gradually increase as the melt continues to evolve to produce the gradational contacts atop magnetite layers. The melt within the boundary layer will also be undercooled with regards to the second phase that crystallizes in the boundary layer to a greater extent directly adjacent to the solidification front compared to the melt located above. This favors the survival of crystals that tend to grow faster parallel to the solidification front, leading to an igneous foliation. It is noted that magnetite layers in the Panzhihua layered intrusion from China sometimes also show similar foliated, plagioclase-bearing layers⁷³ that may have formed in a similar fashion. While the existence of non-cotectic and foliated igneous rocks are generally (and likely correctly) inferred to arise by crystal transport and deposition, magnetite layers of the Bushveld Complex (and potentially some other layered intrusions) present an important case where such features may be produced by in situ crystallization directly at the chamber floor.

Methods

Chemical analysis via a portable XRF spectrometer. In the examples shown in Figs. 4, 5b, magnetite layers were analyzed directly in the drill core from the Rhovan and Vametco vanadium mines using a Niton XL3t portable XRF spectrometer, employing a sample spacing of 2 to 10 cm (Supplementary Data 2)⁷⁴. The instrument analyses an area with a diameter of 8 mm. Each analysis spot was screened with the portable XRF (pXRF) for about 60 s. The instrument was

calibrated once every few hours of its use using its own built-in standards. The following recalculations have been performed to obtain quantitative data from the pXRF. First, the Cr/V ratio of each analysis has been determined. This was done to eliminate any error associated with a potential lack of proper contact between with the pXRF and sample for each analysis. Using a Cr/V ratio also eliminates any feldspar contamination. The recalculated Cr/V ratios are then multiplied by 9.757 for the MML and 20.29 for the BS to obtain a quantitative Cr concentration in weight % that is comparable to in-house XRF analysis on pure magnetite separates. Geochemical data for the pXRF is provided in Supplementary Data 2. Further details regarding the portable XRF analysis and the method used can be found in our previous studies^{13,58}.

Chemical analysis via ICP-MS. The upper gradational contact from the bottom seam shown in Fig. 5c was sampled and cut into 1 cm thick slices in the lower part, and 2-cm-thick slices further upwards. Following crushing and magnetic separation, magnetite was then analyzed via ICP-MS on a Thermo Scientific iCAP RQ at the Earth Lab of the University of the Witwatersrand, South Africa, to quantify its Cr concentration (Supplementary Data 2)⁷⁴. The analytical procedure is given in Supplementary Notes 1. To eradicate potential contamination of feldspar that remained behind after magnetic separation, Cr/Ti ratios are used to construct the geochemical plots. The method still allows to accurately demonstrate the variation in Cr across the magnetite layer since Ti concentrations are generally very constant in a single layer on the scale of the analysis. Plagioclase contamination is eliminated since this mineral contains virtually no Ti or Cr.

Sinking rate of magnetite and plagioclase grains in a magma. The terminal velocity of spherical particles in a fluid can be calculated with the following equation referred to as Stoke's Law:

$$v = 2(\rho_l - \rho_s)gR^2/9\mu$$

where v is the velocity of a solid particle in the fluid in m/s, ρ_l the density of the liquid in kg m^{-3} , ρ_s the density of the solid particle = 2710 kg m^{-3} (plagioclase) and 4800 kg m^{-3} (magnetite), g acceleration due to gravity = 9.8 m s^{-2} , R the radius of the solid particle, and μ the dynamic viscosity of the melt = $10^4 \text{ kg m}^{-1} \text{ s}^{-1}$ (see ref. ⁷⁴). (Supplementary Data 3).

Geochemical modeling. Modeling in Fig. 6 was performed using the Rayleigh fractionation equation based on the lowermost magnetite layer from the Rhovan drill core number PB2009. To determine the bulk-rock partition coefficient for a unit crystallizing magnetite and plagioclase with a gradual increase in the amount of plagioclase crystallization upwards, point counting was performed across the upper gradational contact shown in Fig. 5b. Between 216 and 300 points were counted for each individual sample. Details on the height of the liquid layers from which the magnetite is assumed to have crystallized from and the partition

coefficients chosen for the modeling can be found in the text and Supplementary Data 4⁷⁴.

MELTS modeling. To demonstrate the evolution of a melt that becomes enriched and eventually saturated in plagioclase due to the fractional crystallization of magnetite, modeling was performed using alphaMELTS software, version 1.4.1. Details regarding the MELTS can be found in Supplementary Data 5⁷⁴.

Data availability

All geochemical and textural data, as well as spreadsheets used for geochemical modeling in this study, can be accessed in the online version of this paper or at https://figshare.com/articles/dataset/Supplementary_data_for_paper_In_situ_crystallization_of_foliated_non-cotectic_rocks_on_a_magma_chamber_floor/20510046.

Received: 28 January 2022; Accepted: 12 October 2022;

Published online: 28 October 2022

References

- Wager, L. R. & Brown, G. M. *Layered Igneous Rocks* (Oliver & Boyd, 1968).
- Cawthorn, R. G. (ed.) *Layered intrusions. in Developments in Petrology 15* (Elsevier Science B. V., 1996).
- Charlier, B., Namur, O., Latypov, R. & Tegner, C. (eds.) in *Layered Intrusions* (Springer, 2015).
- Namur, O. et al. Igneous layering in basaltic magma chambers. in *Layered Intrusions* (eds. Charlier, B. et al.) 75–152 (Springer, 2015).
- Campbell, I. H. Some problems with Cumulus theory. *Lithos* **11**, 311–323 (1978).
- McBirney, A. R. & Noyes, R. M. Crystallization and layering of the Skaergaard intrusion. *J. Petrol.* **20**, 487–554 (1979).
- Cawthorn, R. G. & McCarthy, T. S. Variations in Cr content of magnetite from the Upper Zone of the Bushveld Complex—evidence for heterogeneity and convection currents in magma chambers. *Earth. Planet. Sci. Lett.* **46**, 335–343 (1980).
- Cawthorn, R. G. & McCarthy, T. S. Bottom crystallization and diffusion control in layered complexes: evidence from Cr distribution in magnetite from the Bushveld Complex. *Trans. Geol. S. Afr.* **84**, 41–50 (1981).
- Marsh, B. D. Solidification fronts and magmatic evolution. *Mineral. Mag.* **60**, 5–40 (1996).
- Marsh, B. D. Dynamics of magmatic systems. *Elements* **2**, 287–292 (2006).
- Marsh, B. D. On some fundamentals of igneous petrology. *Contrib. Mineral. Petrol.* **166**, 665–690 (2013).
- Latypov, R., Chistyakova, S., Namur, O. & Barnes, S. Dynamics of evolving magma chambers: textural and chemical evolution of cumulates at the arrival of a new liquidus phase. *Earth-Sci. Rev.* **210**, 103388 (2020).
- Kruger, W. & Latypov, R. Fossilized solidification fronts in the Bushveld Complex argue for liquid-dominated magmatic systems. *Nat. Commun.* **11**, 2909 (2020).
- Holness, M. B., Morris, C., Vukmanovic, Z. & Morgan, D. J. Insights into magma chamber processes from the relationship between fabric and grain shape in troctolite cumulates. *Front. Earth. Sci.* **8**, 325 (2020).
- Latypov, R. et al. Chromitite layers indicate the existence of large, long-lived, and entirely molten magma chambers. *Sci. Rep.* **12**, 4092 (2022).
- Latypov, R. & Chistyakova, S. Origin of non-cotectic cumulates: a novel approach. *Geology* **48**, 604–608 (2020).
- Cawthorn, R. G. Delayed accumulation of plagioclase in the Bushveld Complex. *Mineral. Mag.* **66**, 881–893 (2006).
- Jenkins, M. C. & Mungall, J. E. Genesis of the Peridotite Zone, Stillwater Complex, Montana, USA. *J. Petrol.* **59**, 2157–2189 (2018).
- Higgins, M. D. The origin of laminated and massive anorthosite, Sept Iles layered intrusion, Quebec, Canada. *Contrib. Mineral. Petrol.* **106**, 340–354 (1991).
- Jackson, E. D. Primary textures and mineral associations in the Ultramafic Zone of the Stillwater Complex, Montana. *U. S. Geol. Surv. Prof. Pap.* **358**, 108 (1961).
- Cawthorn, R. G. & Ashwal, L. D. Origin of anorthosite and magnetite layers in the Bushveld Complex, constrained by major element compositions of plagioclase. *J. Petrol.* **50**, 1607–1637 (2009).
- Hess, H. H. Stillwater igneous complex, Montana. *Geol. Soc. Am. Memoir.* **80**, 1–230 (1960).
- Namur, O. et al. Anorthosite formation by plagioclase flotation in ferrobasalt and implications for the lunar crust. *Geochem. Cosmochim. Acta.* **75**, 4998–5018 (2011).
- Meurer, W. P. & Boudreau, A. E. Compaction of igneous cumulates part II: compaction and the development of igneous foliations. *J. Geol.* **106**, 293–304 (1998).
- O'Driscoll, B. et al. Magmatic lineations inferred from anisotropy of magnetic susceptibility fabrics in Units 8, 9, and 10 of the Rum Eastern Layered Series, NW Scotland. *Lithos* **98**, 27–44 (2007).
- Barnes, S. J., Latypov, R., Chistyakova, S., Godel, B. & Schoneveld, L. E. Idiomorphic oikocrysts of clinopyroxene produced by a peritectic reaction within a solidification front of the Bushveld. *Complex. Contrib. Mineral. Pet.* **176**, 5 (2021).
- Holness, M. B. et al. Crystal mush growth and collapse on a steep wall: the Marginal Border Series of the Skaergaard intrusion, East Greenland. *J. Petrol.* **63**, 1–21 (2022).
- Scoon, R. N. & Mitchell, A. A. The upper zone of the Bushveld Complex at Roosenekal, South Africa: geochemical stratigraphy and evidence of multiple episodes of magma replenishment. *S. Afr. J. Geol.* **115**, 515–534 (2012).
- Yuan, Q. et al. Pulses of plagioclase-laden magmas and stratigraphic evolution in the upper zone of the Bushveld Complex, South Africa. *J. Petrol.* **58**, 1619–1644 (2017).
- Yao, Z., Mungall, J. E. & Jenkins, M. C. The Rustenburg Layered Suite formed as a stack of mush with transient magma chambers. *Nat. Commun.* **12**, 505 (2021).
- Maier, W. D., Barnes, S. J. & Groves, D. I. The Bushveld Complex, South Africa: formation of platinum-palladium, chrome- and vanadium-rich layers via hydrodynamic sorting of a mobilized cumulate slurry in a large, relatively slowly cooling, subsiding magma chamber. *Miner. Depos.* **48**, 1–56 (2013).
- Vukmanovic, Z., Holness, M. B., Monks, K. & Anderson, J. C. Ø. The Skaergaard trough layering: sedimentation in a convecting magma chamber. *Contrib. Mineral. Petrol.* **173**, 43 (2018).
- Cawthorn, R. G. Growth nodes at the base of magnetite layers in the upper zone of the Bushveld Complex. *S. Afr. J. Geol.* **97**, 455–461 (1994).
- Kruger, F. J. & Smart, R. Diffusion of trace elements during bottom crystallization of double-diffusive convection systems: the magnetite layers of the Bushveld Complex. *J. Volcanol. Geotherm.* **34**, 133–142 (1987).
- Irving, A. J. A review of experimental studies of crystal/liquid trace element partitioning. *Geochem. Cosmochim. Acta.* **42**, 743–770 (1978).
- Toplis, M. J. & Corgne, A. An experimental study of element partitioning between magnetite, clinopyroxene and iron-bearing silicate liquids with particular emphasis on vanadium. *Contrib. Mineral. Petrol.* **144**, 22–37 (2002).
- Bachmann, O., Dungan, M. A. & Bussy, F. Insights into shallow magmatic processes in large silicic magma bodies: the trace element record in the Fish Canyon magma body, Colorado. *Contrib. Mineral. Petrol.* **149**, 338–349 (2004).
- Dare, A. S., Barnes, S.-J. & Beaudoin, G. Variation in trace element content of magnetite crystallized from a fractionating sulfide liquid, Sudbury, Canada: implications for provenance discrimination. *Geochem. Cosmochim. Acta.* **88**, 27–50 (2012).
- Castle, N. & Herd, C. D. K. Experimental petrology of the Tissint meteorite: redox estimates, crystallization curves, and evaluation of petrogenetic models. *Meteorit. Planet. Sci.* **52**, 125–146 (2017).
- Siewwright, R. H., St O'Niell, H. C., Tolley, J., Wilkinson, J. J. & Barry, A. J. Diffusion and partition coefficients of minor and trace elements in magnetite as a function of oxygen fugacity at 1150 °C. *Contrib. Mineral. Petrol.* **175**, 40 (2020).
- Yao, Z. & Mungall, J. E. Magnetite layer formation in the Bushveld Complex of South Africa. *Nat. Commun.* **13**, 416 (2022).
- Cawthorn, R. G. & Street, J. Vertical migration of residual magma in the upper zone of the Bushveld Complex. *Mineral. Petrol.* **51**, 345–354 (1994).
- Cawthorn, R. G. The Bushveld Complex. in *Layered Intrusions* (eds. Charlier, B. et al.) 517–587 (Springer, 2015).
- Cawthorn, R. G. The residual or roof zone of the Bushveld Complex, South Africa. *J. Petrol.* **54**, 1875–1900 (2013).
- McCarthy, T. S. & Cawthorn, R. G. The geochemistry of vanadiferous magnetite in the Bushveld Complex: implications for crystallization mechanisms in layered complexes. *Mineral. Deposita.* **18**, 505–518 (1983).
- McCarthy, T. S., Cawthorn, R. G., Wright, C. J. & McIver, J. R. Mineral layering in the Bushveld Complex: implications of Cr abundances in magnetite from closely spaced magnetite and intervening silicate-rich layers. *Econ. Geol.* **80**, 1062–1074 (1985).
- Irvine, T. N. & Smith, C. H. Primary oxide minerals in the layered series of the Muskox intrusion. in *Magmatic Ore Deposits* (eds. Wilson, H. D. B.) 77–96 (Society of Economic Geologists, 1969).
- Cawthorn, R. G. & Molyneux, T. S. Vanadiferous magnetite deposits of the Bushveld Complex. in *Mineral deposits of Southern Africa* (ed. Anheuser, C. R.) 1251–1266 (Geological Society of South Africa, 1986).
- Cawthorn, R. G., Barnes, S. J., Ballhaus, C. & Malitch, K. N. Platinum group element, chromium, and vanadium deposits in mafic and ultramafic rocks. *Econ. Geol.* **100**, 215–249 (2005).

50. Toplis, M. J. & Carroll, M. R. An experimental study of the influence of oxygen fugacity on Fe-Ti oxide stability, phase relations, and mineral-melt equilibria in ferro-basaltic systems. *J. Petrol.* **36**, 1137–1170 (1995).
51. Molyneux, T. C. X-ray-data and chemical analysis of some titanomagnetite and ilmenite samples from the Bushveld Complex, South Africa. *Mineral. Mag.* **38**, 863–871 (1972).
52. Cawthorn, R. G. Genesis of magmatic oxide ore deposits—a view from the Bushveld Complex. *Norges Geol. Undersøk. Spec. Publ.* **9**, 11–21 (2003).
53. Cawthorn, R. G., McCarthy, T. S. & Davies, G. Vertical chemical gradients in a single grain of magnetite from the Bushveld Complex, South Africa. *Mineral. Mag.* **47**, 27–34 (1983).
54. Reynolds, I. M. The nature and origin of titaniferous magnetite-rich layers in the Upper Zone of the Bushveld Complex: a review and synthesis. *Econ. Geol.* **80**, 1089–1108 (1995).
55. Morse, S. A. Convection in aid of adcumulus growth. *J. Petrol.* **27**, 1183–1214 (1986).
56. Tegner, C., Cawthorn, R. G. & Kruger, F. J. Cyclicity in the main and upper zones of the Bushveld Complex, South Africa: crystallization from a zoned magma sheet. *J. Petrol.* **47**, 2257–2279 (2006).
57. Maila, R. P. *Geochemistry of Magnetite Layers in the Upper Zone of the Bushveld Complex, South Africa*. Thesis, Univ. Witwatersrand (2015).
58. Kruger, W. & Latypov, R. Magmatic karst reveals dynamics of crystallization and differentiation in basaltic magma chambers. *Sci. Rep.* **11**, 7341 (2021).
59. Latypov, R. et al. Platinum-bearing chromite layers are caused by pressure reduction during magmatic ascent. *Nat. Commun.* **9**, 462 (2018).
60. Vukmanovic, Z., Holness, M. B., Stock, M. J. & Roberts, R. J. The creation and evolution of crystal mush in the Upper Zone of the Rustenburg Layered Suite, South Africa. *J. Petrol.* **60**, 1523–1542 (2019).
61. Martin, D., Griffiths, R. W. & Campbell, I. H. Compositional and thermal convection in magma chambers. *Contrib. Mineral. Petrol.* **96**, 465–475 (1987).
62. Campbell, I. H. Fluid dynamic processes in basaltic magma chambers. in *Layered Intrusions* (ed. Cawthorn, R. G.) 45–76 (Developments in Petrology 15, Elsevier Science BV, 1996).
63. Seedhouse, J. K. & Donaldson, C. H. Compositional convection caused by olivine crystallization in a synthetic basalt melt. *Mineral. Mag.* **60**, 115–130 (1996).
64. Huppert, H. E. & Sparks, J. S. The fluid dynamics of a basaltic magma chamber replenished by influx of hot, dense, ultrabasic magma. *Contrib. Mineral. Petrol.* **75**, 279–289 (1980).
65. Maaløe, S. The zoned plagioclase of the Skaergaard intrusion, East Greenland. *J. Petrol.* **17**, 398–419 (1976).
66. Boorman, S., Boudreau, A. & Kruger, F. J. The lower zone-critical zone transition of the Bushveld Complex: a quantitative textural study. *J. Petrol.* **45**, 1209–1235 (2004).
67. O'Driscoll, B., Donaldson, C. H., Troll, V. R., Jerram, D. A. & Emeleus, C. H. An origin for harristic and granular olivine in the Rum layered series, NW Scotland: a crystal size distribution study. *J. Petrol.* **48**, 253–270 (2007).
68. Robins, B. Crescumulate layering in a gabbroic body on Seiland, northern Norway. *Geol. Mag.* **109**, 533–542 (1973).
69. Wadsworth, W. J. The layered ultrabasic rocks of south-west Rhum, Inner Hebrides. *Phil. Trans. Royal Soc. Lond.* **244**, 21–64 (1961).
70. Smith, J. V. & Brown, W. L. *Feldspar minerals. Volume 1. Crystal Structures, Physical, Chemical, and Microtextural Properties* (Springer-Verlag, 1988).
71. Howarth, G. H., Prevec, S. A. & Zhou, M. F. Timing of Ti-magnetite crystallization and silicate disequilibrium in the Panzihua mafic layered intrusion: implications for ore forming processes. *Lithos* **170**, 73–89 (2013).
72. Kruger, W. Supplementary data for paper In situ crystallization of foliated, non-cotectic rocks on a magma chamber floor. figshare. <https://doi.org/10.6084/m9.figshare.20510046.v1> (2022).
73. Donaldson, C. H. Convective fractionation during magnetite and hematite dissolution in silicate melts. *Mineral. Mag.* **57**, 469–488 (1993).
74. Roeder, P. L. & Osborn, E. F. Experimental data for the system MgO-FeO-Fe₂O₃-CaAl₂Si₂O₈ and their petrologic implications. *Am. J. Sci.* **264**, 428–480 (1966).

Acknowledgements

The original manuscript benefited from constructive reviews by Grant Cawthorn, Steve Barnes, Olivier Namur, and two anonymous reviewers. The staff members from the Rhovan and Vametco vanadium mines are thanked for allowing access to their drill cores. The study was supported by research grants to W.K. and R.L. from the National Research Foundation (NRF) and the Department of Science and Technology (DST)-NRF Center of Excellence for Integrated Mineral and Energy Resource Analysis (CIMERA) of South Africa. Any opinion, finding and conclusion or recommendation expressed in this contribution is that of the authors and the DST-NRF CIMERA and NRF do not accept any liability in this regard.

Author contributions

W.K. performed analytical work and wrote the first draft of the paper. W.K. and R.L. both contributed to the interpretation of data, formulating the original idea, and writing the final version of the paper.

Competing interests

The authors declare no competing interests.

Additional information

Supplementary information The online version contains supplementary material available at <https://doi.org/10.1038/s43247-022-00584-6>.

Correspondence and requests for materials should be addressed to Willem Kruger.

Peer review information *Communications Earth & Environment* thanks Stephen Prevec and Frank Tepely for their contribution to the peer review of this work. Primary Handling Editor: Joe Aslin. Peer reviewer reports are available.

Reprints and permission information is available at <http://www.nature.com/reprints>

Publisher's note Springer Nature remains neutral with regard to jurisdictional claims in published maps and institutional affiliations.



Open Access This article is licensed under a Creative Commons Attribution 4.0 International License, which permits use, sharing, adaptation, distribution and reproduction in any medium or format, as long as you give appropriate credit to the original author(s) and the source, provide a link to the Creative Commons license, and indicate if changes were made. The images or other third party material in this article are included in the article's Creative Commons license, unless indicated otherwise in a credit line to the material. If material is not included in the article's Creative Commons license and your intended use is not permitted by statutory regulation or exceeds the permitted use, you will need to obtain permission directly from the copyright holder. To view a copy of this license, visit <http://creativecommons.org/licenses/by/4.0/>.

© The Author(s) 2022